# Selective inactivation of Gram-positive bacteria *in vitro* and *in vivo* through metabolic labelling

Tao Feng[1†*], Hui Lu[1†], Xiaoting Ye[1†], Chaofan Nie[1], Jianhong Zhang[1], Luofeng Yu[1], Haoyu Jin[1], Peng Li[1*] and Wei Huang[1,2,3]

**ABSTRACT** Bacterial infections are grave threats to human health, particularly those caused by the most common Gram-positive bacteria. The massive administration of broad-spectrum antibiotics to treat various bacterial infections has led to the evolution and spread of drug resistance. As a universal antimicrobial technique unapt to induce drug resistance, photothermal therapy (PTT) is attracting extensive attention in recent years. However, its unspecific killing capability and side effects towards adjacent mammalian cells severely impede the practical applications. Herein, we proposed a metabolic engineering strategy to selectively inactivate Gram-positive bacteria by PTT. A bioorthogonal photothermal agent was prepared by the conjugation of IR-780 iodide and dibenzocyclooctyne (IR780-DBCO). Upon pre-metabolizing with 3-azido-D-alanine, Gram-positive bacteria rather than Gram-negative ones, such as *Staphylococcus aureus* and vancomycin-resistant *Enterococcus faecalis* (VRE), could be specifically tied up by the explosive IR780-DBCO *via* copper-free click chemistry. Thereafter, they spontaneously detonated under 15 min near-infrared light irradiation and inactivated nearly 100% Gram-positive bacteria *in vitro*. Moreover, superbug VRE-induced infection was significantly inhibited by this approach in a mouse skin wound model. This metabolic labelling-based photothermal ablation strategy specific to Gram-positive microbes would stimulate the development of precise antibacterial candidates for preclinical applications.

**Keywords:** Gram-positive bacteria, selective inactivation, photothermal agent, metabolic labelling, wound infection

## INTRODUCTION

Bacterial infectious diseases are severe challenges to human health, leading to significantly social and medical concerns for a long time [1,2]. As a primary category of clinically significant pathogens, Gram-positive bacteria induce serious infections with high morbidity and mortality [3,4], such as sepsis that annually accounts for nearly 1.7 million cases and 270,000 deaths in the United States, as well as 30 million cases and 6 million deaths all around the world [5,6]. Generally, bacterial infections are cured by broad-spectrum antibiotics, while their global overuse or abuse has accelerated the evolution and spread of drug resistance [7–9]. In addition, this situation is deteriorated as the production of novel antimicrobial agents is increasingly difficult and costly [10]. As reported by the World Health Organization (WHO), the drug-resistant bacterial infections claim more than 700,000 lives every year, and if current trends continue, the number could rise to 10 million by 2050 with an estimated economic cost of 100 trillion dollars [11,12]. Therefore, it is highly desirable to develop effective antimicrobial agents incapable of inducing drug resistance in the post-antibiotic era, especially those specific to Gram-positive bacteria [13].

Recently, photothermal therapy (PTT) has attracted extensive attention for bactericidal applications, on the basis of generating localized hyperthermia to inactivate enzymes or proteins, disrupt membrane permeability, and disorder metabolic signals upon near-infrared (NIR) light irradiation with photothermal agents [14–17]. PTT holds advantageous characteristics of spatiotemporal control, noninvasiveness, and little possibility to induce drug resistance. Up to now, various photothermal agents have been developed to ablate bacteria, including inorganic gold-silver nanocages, copper sulfide, graphene, and black phosphorus, as well as organic IR-780 iodide (IR780), indocyanine green, polydopamine, and polypyrrole [18–22]. However, PTT suffers from the inability to specifically inactivate bacteria and toxic side effects against adjacent mammalian cells, which seriously limit its practical usage.

Metabolic labelling with unnatural precursors is an emerging technique to engineer cells with chemical tags for subsequent modification of complementary molecules *via* efficient chemistries [23–25], which has been extensively applied in various fields, including cancer labelling and targeting [24], microbiota identification [26–28], and bacterial inactivation [29–31]. A variety of artificial precursors such as chemically modified galactosamine, mannosamine, sialic acid, and fucose are used for cell membrane labelling. Benefitting from the specific components of bacterial cell wall, D-alanine and 3-deoxy-D-manno-octulosonic acid derivatives are metabolized into the peptidoglycan and lipopolysaccharide, respectively [32,33]. There-

[1] Frontiers Science Center for Flexible Electronics (FSCFE), Xi'an Institute of Flexible Electronics (IFE), Xi'an Institute of Biomedical Materials and Engineering (IBME), Ningbo Institute & Chongqing Technology Innovation Center, Northwestern Polytechnical University (NPU), Xi'an 710072, China
[2] Key Laboratory of Flexible Electronics (KLOFE) & Institute of Advanced Materials (IAM), Nanjing Tech University (NanjingTech), Nanjing 211816, China
[3] Key Laboratory for Organic Electronics and Information Displays & Institute of Advanced Materials (IAM), Nanjing University of Posts and Telecommunications, Nanjing 210023, China
† These authors contributed equally to this work.
* Corresponding authors: (emails: iampli@nwpu.edu.cn (Li P); iamtfeng@nwpu.edu.cn (Feng T))

after, functional fluorescent probes and therapeutic molecules are introduced by bioorthogonal reactions, such as click chemistry between azide and alkyne [31,34]. Thus, metabolic labelling could be utilized to precisely conjugate photothermal agents on bacteria for selective pathogenic ablation by PPT.

In this contribution, IR780, a lipophilic cationic heptamethine dye with excellent degradability, low cytotoxicity, and superior photothermal conversion efficiency [35–37], was functionalized with dibenzocyclooctyne (DBCO) to prepare a bioorthogonal photothermal agent (IR780-DBCO) for specific killing of Gram-positive bacteria *in vitro* and *in vivo* (Fig. 1). Upon metabolizing 3-azido-*D*-alanine (*D*-Ala-$N_3$) into bacterial peptidoglycan, IR780-DBCO was selectively labelled on the surface of Gram-positive bacteria rather than Gram-negative ones *via* copper-free click chemistry between azide and DBCO. The specific labelling resulted from the poor permeability of Gram-negative bacterial outer membrane against IR780-DBCO with a molecular weight larger than 650 Da [31,38]. Therefore, typical Gram-positive pathogenic bacteria, including *Staphylococcus aureus* (*S. aureus*) and vancomycin-resistant *Enterococcus faecalis* (VRE), were selectively ablated under NIR light irradiation *in vitro* and *in vivo*.

## EXPERIMENTAL SECTION

### Materials and characterizations
The experimental details of materials, characterizations, synthesis of IR780-(3-MPA) and IR780-DBCO, photothermal heating curves measurement, bacteria culture and metabolic modification, morphology observation, cytotoxicity and hemolysis assays are described in the Supplementary information.

### Bacterial labelling
One milliliter of *D*-Ala-$N_3$-pretreated or unpretreated bacterial suspension (*S. aureus*, VRE, *Escherichia coli* (*E. coli*), or *Pseudomonas aeruginosa* (*P. aeruginosa*)) in a 1.5-mL Eppendorf tube was centrifuged at 2300 ×*g* for 5 min. After the supernatant was discarded, bacteria were resuspended in 200 μL of DBCO-

Cy3 solution (20 μmol $L^{-1}$, phosphate buffer saline (PBS)/dimethyl sulfoxide (DMSO) (*v/v*) = 99/1) and incubated at room temperature in the dark for 30 min. The labelled bacteria were harvested and washed with PBS for four times. Upon fixing in 1 mL of 4% paraformaldehyde at 4°C overnight, the bacteria were collected and washed with PBS for four times. Then 1 mL PBS was added to resuspend the labelled bacteria. The above bacterial suspension (10 μL) was transferred into a confocal dish and covered by a clean cover glass for imaging. The images were recorded by an inverted fluorescence microscope with excitation wavelength of 530 nm and emission wavelength of 593 nm, and a structured illumination microscope (SIM) with excitation wavelength of 561 nm and emission wavelength of 600–660 nm.

### *In vitro* selective antibacterial assays
The antibacterial activity of IR780-DBCO towards *S. aureus*, VRE, *E. coli*, or *P. aeruginosa* was evaluated by a standard agar plating method. First, 1 mL of the pretreated bacteria in a 1.5-mL Eppendorf tube was centrifuged at 2300 ×*g* for 5 min to discard the supernatant. Second, the bacteria were suspended in 200 μL of IR780-DBCO solutions with various concentrations (0, 2.5, 5, or 10 μmol $L^{-1}$, PBS/DMSO (*v/v*) = 99/1), and incubated at room temperature in the dark for 30 min. Then the labelled bacteria were harvested and washed with PBS for three times, and subsequently resuspended in 400 μL PBS. For the antibacterial activity of IR780-DBCO under NIR light irradiation, 200 μL of the above-prepared bacterial suspension was transferred to a sterile disposable petri dish and irradiated by 808-nm NIR laser (1.0 W $cm^{-2}$) for 15 min. For the antibacterial activity of IR780-DBCO in the dark, 200 μL of the above-prepared bacterial suspension was placed in the dark for 15 min under the same conditions. Afterwards, 1.8 mL PBS was added to the petri dish, followed by sonication for 3 min to disperse the bacteria. One hundred microliter of the suspension was taken for 10-fold gradient dilution. Ten microliter of the diluted bacterial solution was inoculated in an agar plate, and the colony forming units (CFUs) were counted after incubation at 37°C overnight. In addition, 50 μL of the suspension diluted by 100 folds was spread
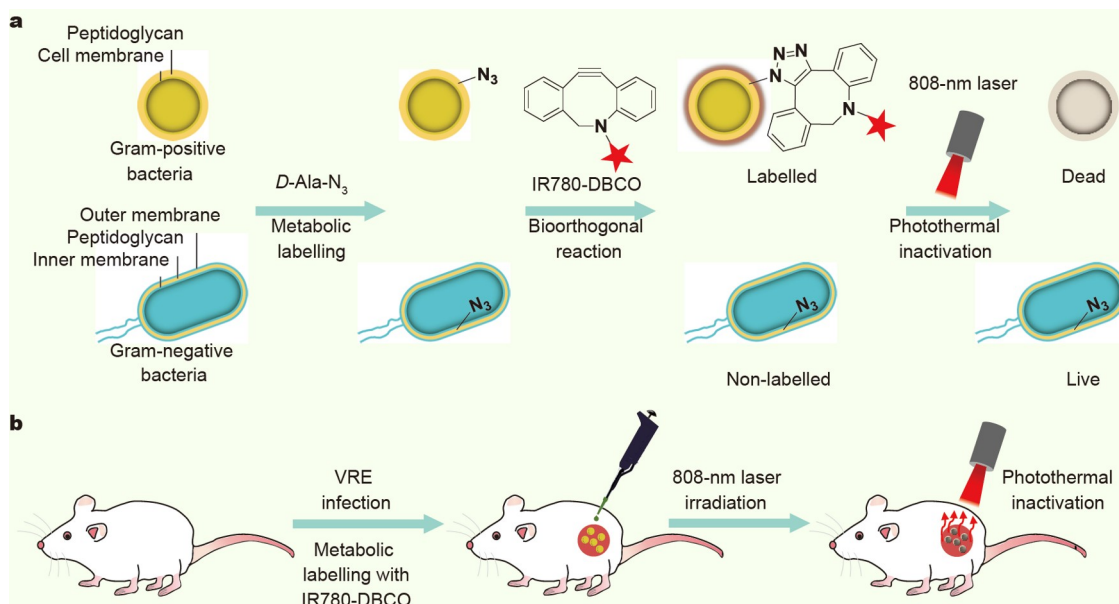


**Figure 1**  Schematic illustration of IR780-DBCO for selective photothermal inactivation of Gram-positive bacteria (a) *in vitro* and (b) *in vivo*.

on the agar plate. The bacterial viability (%) = $CFU_{experiment}$/$CFU_{control}$ × 100%, where $CFU_{experiment}$ and $CFU_{control}$ were the average CFU of the experimental group with IR780-DBCO treatment and the control group with PBS treatment, respectively. All experiments were repeated for three times. Using the similar method, the antibacterial activity of IR780-DBCO (0 and 5 μmol $L^{-1}$, PBS/DMSO ($v/v$) = 99/1) towards *S. aureus*, VRE, *E. coli*, or *P. aeruginosa* without D-Ala-$N_3$ pretreatment was evaluated in the dark or under NIR laser irradiation. In addition, the killing effect of IR780, IR780-(3-MPA), or IR780-DBCO (0 and 5 μmol $L^{-1}$, PBS/DMSO ($v/v$) = 99/1) against D-Ala-$N_3$-pretreated or unpretreated VRE was measured in the dark or under NIR light illumination.

### *In vivo* anti-infective assay

The *in vivo* anti-infective ability of IR780-DBCO was assessed in a mouse model with VRE-infected wound. All procedures were approved by the Animal Ethical Committee of Northwestern Polytechnical University. Female BALB/c mice (6–8 weeks) were purchased from Beijing Vital River Laboratory Animal Technology Co., Ltd.

Twelve BALB/c mice were randomly divided into four groups: (1) control group only with bacterial infection, (2) bacteria-infected group under 808-nm NIR laser irradiation, (3) bacteria-infected group treated with IR780-DBCO, and (4) bacteria-infected group treated with IR780-DBCO and 808-nm NIR laser irradiation. The mice were anesthetized using isoflurane and then the open excision wounds were created on the dorsal skin using an 8-mm diameter biopsy punch. The bacteria-infected skin wound models were established by inoculating 50 μL of the pretreated VRE suspension ($10^4$ CFU) on the wound area. For the groups with IR780-DBCO treatment, a total of 50 μL of the pretreated VRE suspension and IR780-DBCO (the final concentration was 20 μmol $L^{-1}$) were added onto each wound and kept for 30 min. Afterwards, the wounds were irradiated by 808-nm NIR laser (1.0 W $cm^{-2}$) for 15 min or kept in the dark. The treatments by IR780-DBCO and with or without 808-nm NIR laser irradiation were performed for total three times. The wound areas were photographed using an 8-mm rubber ring as reference every day. After four days, the mice were sacrificed and the entire wounds with the adjacent skin tissues were harvested and placed in 1 mL PBS followed by sonication for 15 min. The CFUs of bacteria in infectious tissues were evaluated by the standard agar plating method. The collected wound tissues were fixed in 4% paraformaldehyde at 4°C, embedded in paraffin, and cut into slices for histopathological hematoxylin-eosin (H&E) staining.

## RESULTS AND DISCUSSION

### Synthesis and characterization of IR780-DBCO

To enable photothermal property and the reactivity with azide group, IR780 was firstly conjugated with 3-mercaptopropionic acid (3-MPA) through nucleophilic substitution reaction between sulfhydryl and chlorine groups to produce IR780-(3-MPA) in a 64% yield, and subsequently reacted with DBCO-amine (DBCO-$NH_2$) through amide condensation reaction to prepare IR780-DBCO in a 43% yield (Fig. S1 and Fig. 2a). As confirmed by nuclear magnetic resonance and mass spectra, IR780-DBCO was successfully synthesized. The optical characteristic of IR780-DBCO was displayed in Fig. 2b, with the absorption lying in the broad ultra violet-visible-NIR (UV-Vis-NIR) range from 200 to 900 nm and the maximal peak located at 785 nm. Moreover, the temperature evolution curves of IR780-
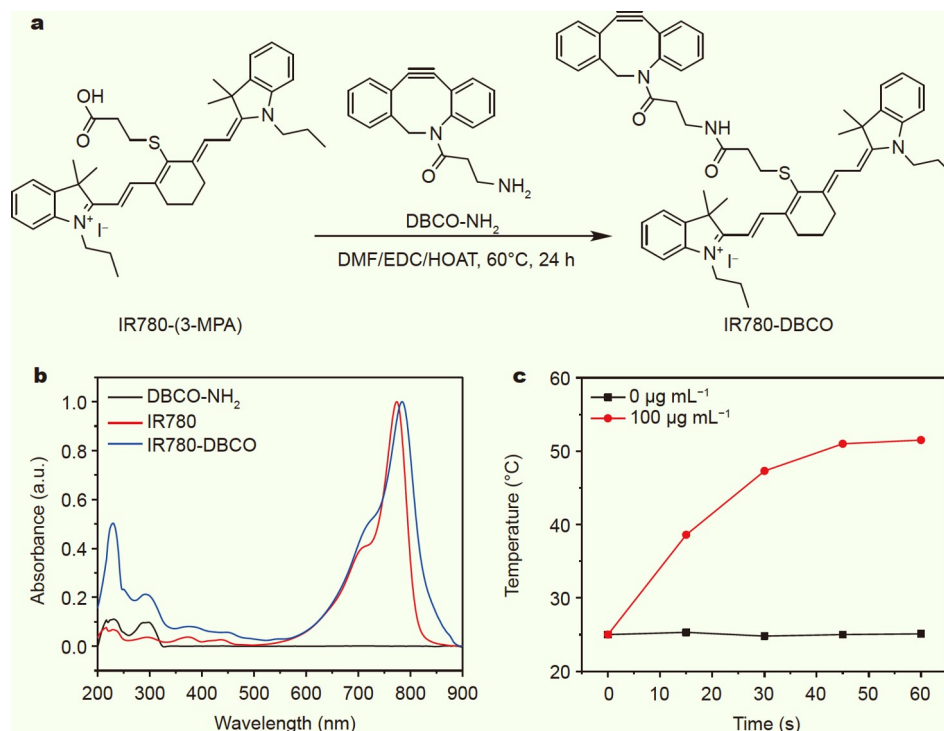


**Figure 2** (a) Synthetic route of IR780-DBCO. (b) UV-Vis-NIR absorption spectra of DBCO-$NH_2$, IR780, and IR780-DBCO in DMSO/PBS mixtures ($v/v$ = 1/99). DMF: *N,N*-dimethylformamide; EDC: 1-(3-dimethylaminopropyl)-3-ethylcarbodiimide hydrochloride; HOAT: 1-hydroxy-7-azabenzotriazole. (c) Temperature evolution curves of IR780-DBCO at different concentrations (0 and 100 μg $mL^{-1}$) under NIR laser irradiation (808 nm, 1.0 W $cm^{-2}$) for 60 s.

DBCO were measured under 808-nm NIR laser irradiation with a power density of $1.0\,W\,cm^{-2}$ (Fig. 2c). At a concentration of $100\,\mu g\,mL^{-1}$, the temperature increased by 26.5°C upon irradiation for 60 s, while it had negligible change at $0\,\mu g\,mL^{-1}$ under the same condition. Upon IR780-DBCO reacting with $D$-Ala-N$_3$ through click chemistry, there were no significant differences for the UV-Vis-NIR spectrum and temperature evolution curve when compared with those for IR780-DBCO alone (Fig. S2). These results revealed that IR780-DBCO possessed an outstanding photothermal effect, which was not influenced by the click reaction, and held great potential for eliminating bacteria.

**Selective bacterial labelling**
In order to evaluate the specific labelling of Gram-positive bacteria by metabolic engineering, two Gram-positive bacteria (*S. aureus* and VRE) and two Gram-negative bacteria (*E. coli* and *P. aeruginosa*) were pretreated with $D$-Ala-N$_3$ to integrate azide groups into the peptidoglycan of bacteria, followed by bioorthogonal clicking with fluorescent DBCO-Cy3, a commercial dye containing alkyne groups. As shown in Fig. 3, Gram-positive *S. aureus* and VRE were stained with strong red fluorescence, while Gram-negative *E. coli* and *P. aeruginosa* presented almost no fluorescence. Without pretreatment with $D$-Ala-N$_3$, all types of bacteria showed negligible fluorescence, indicating the efficient click reaction between DBCO-Cy3 and metabolic precursor (Fig. S3). Most importantly, to demonstrate the exact region of labelled DBCO-Cy3, super resolution imaging of bacteria was performed by SIM. The obvious fluorescence was only observed around the periphery of Gram-positive bacteria (*S. aureus* and VRE), indicating the preferential labelling of their cell walls (Fig. 4). The underlying mechanism for selective imaging of Gram-positive bacteria could be explained as follows: $D$-Ala-N$_3$ was able to metabolize into peptidoglycan of bacterial cell wall to endow azide groups owing to the presence of $D$-alanine motif [32]. The outer membrane of Gram-negative bacteria is less permeable to molecules with molecular weight larger than 650 Da [31], and thus DBCO-Cy3 with molecular weight of 1186 Da was specifically labelled on Gram-positive bacteria through copper-free click chemistry between azide and DBCO groups. Moreover, while traditional culture-based methods for bacterial identification usually require several days, this metabolic labelling approach is much faster and effective.

**Photothermal antibacterial study**
Because of the similar chemical structure to DBCO-Cy3, IR780-DBCO with a molecular weight of 994 Da could be specifically loaded on the cell envelope of $D$-Ala-N$_3$-pretreated Gram-positive bacteria, which is advantageous for photothermal inactivation of pathogens. We then assessed the selective antibacterial capability of IR780-DBCO using the standard plate counting method [20]. Gram-positive bacteria (*S. aureus* and VRE) and Gram-negative ones (*E. coli* and *P. aeruginosa*) were metabolized with $D$-Ala-N$_3$ and incubated with IR780-DBCO at different concentrations, followed by treatment in dark or under 808-nm NIR laser irradiation at a power density of $1.0\,W\,cm^{-2}$ for 15 min. For Gram-positive bacteria, IR780-DBCO showed concentration-dependent inhibition under NIR light irradiation, with the killing efficiency of 99.7% for *S. aureus* or 100% for VRE, and few bacterial colonies formed on the agar plates at a concentration of $10\,\mu mol\,L^{-1}$ (Fig. 5a–d). Nevertheless, NIR light irradiation or IR780-DBCO alone presented negligible killing effect on Gram-positive bacteria, which grew smoothly on the agar plates. For Gram-negative bacteria, the killing effect was insignificant upon treatment with NIR light irradiation, IR780-DBCO, or IR780-DBCO plus NIR light irradiation, resulting in obvious colony formation similar to the control group (Fig. 5e–h). Without $D$-Ala-N$_3$ pretreatment, the viability of all types of bacteria was much higher upon incubation with equivalent IR780-DBCO or plus NIR light irradiation (Fig. S4). Moreover,
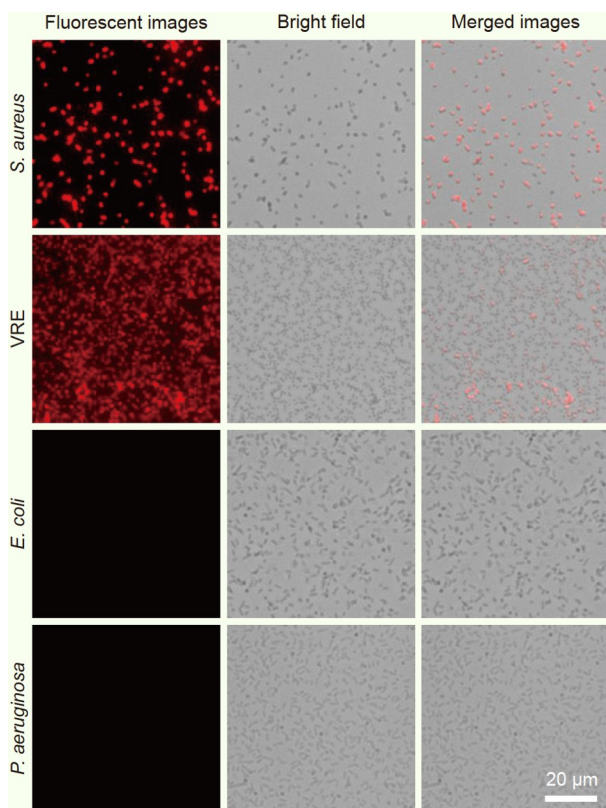


**Figure 3** Fluorescent images of Gram-positive bacteria (*S. aureus* and VRE) and Gram-negative bacteria (*E. coli* and *P. aeruginosa*) upon incubation with $D$-Ala-N$_3$ and DBCO-Cy3. The fluorescent channel was recorded with excitation wavelength of 530 nm and emission wavelength of 593 nm.
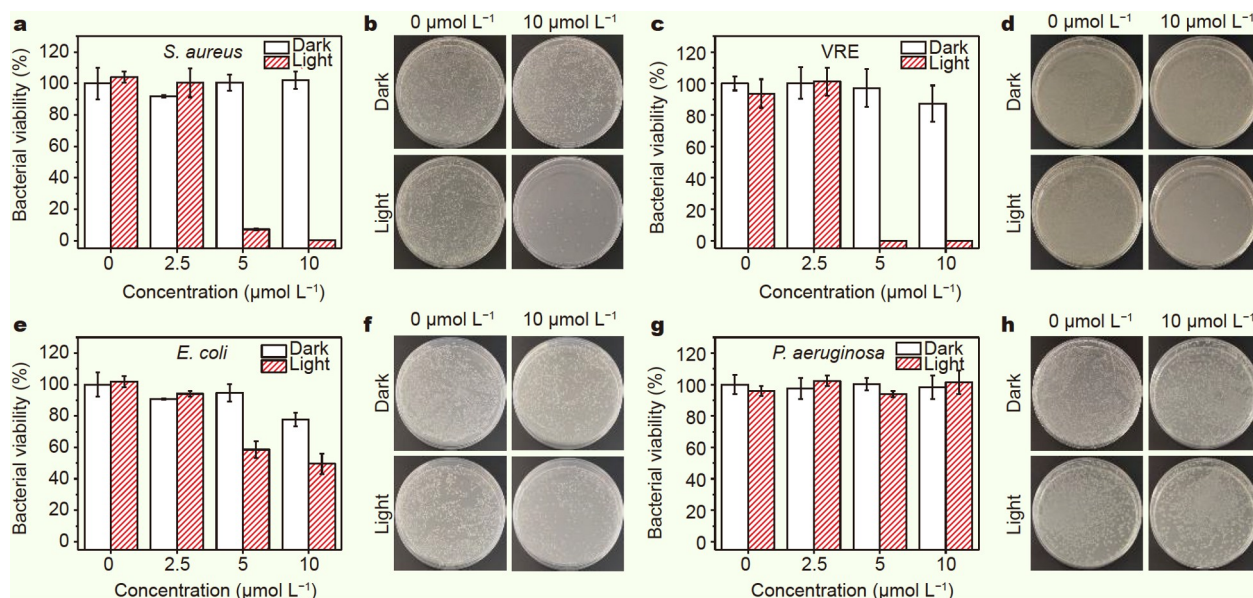


**Figure 4** SIM images of Gram-positive bacteria (*S. aureus* and VRE) and Gram-negative bacteria (*E. coli* and *P. aeruginosa*) upon incubation with $D$-Ala-N$_3$ and DBCO-Cy3. The fluorescence was measured with excitation wavelength of 561 nm and emission wavelength of 600–660 nm.

for Gram-positive VRE, the killing effect of IR780 and IR780-(3-MPA) without or with $D$-Ala-N$_3$ pretreatment was much lower than that incubated with $D$-Ala-N$_3$ and equivalent IR780-DBCO under NIR light illumination (Fig. S5). These results suggested that Gram-positive bacteria rather than Gram-negative ones could be selectively and effectively eliminated by PTT through metabolic labelling of IR780-DBCO on the cell wall.

Moreover, in order to elucidate the antibacterial mechanism, scanning electron microscopy (SEM) was utilized to observe the morphological changes of bacteria after different treatments. Upon metabolic labelling with IR780-DBCO and irradiation with NIR light, the cell envelopes of Gram-positive bacteria were seriously destroyed, with obvious deformation and collapse for $S.$ $aureus$ and obvious wrinkle for VRE, as indicated by the white arrows in Fig. 6 and Fig. S6. However, the morphology of Gram-positive bacteria treated with NIR light irradiation or IR780-DBCO or Gram-negative bacteria with any treatment had insignificant change, displaying intact cell wall and relatively



**Figure 5** (a, c, e, g) Bacterial viability and (b, d, f, h) photographs of the corresponding colonies of $D$-Ala-N$_3$-pretreated Gram-positive bacteria, (a, b) $S.$ $aureus$ and (c, d) VRE, and Gram-negative bacteria, (e, f) $E.$ $coli$ and (g, h) $P.$ $aeruginosa$, upon incubation with IR780-DBCO at various concentrations and irradiation with/without 808-nm laser at a power density of $1.0\,\mathrm{W\,cm^{-2}}$ for 15 min. Error bars: mean $\pm$ SD ($n = 3$).
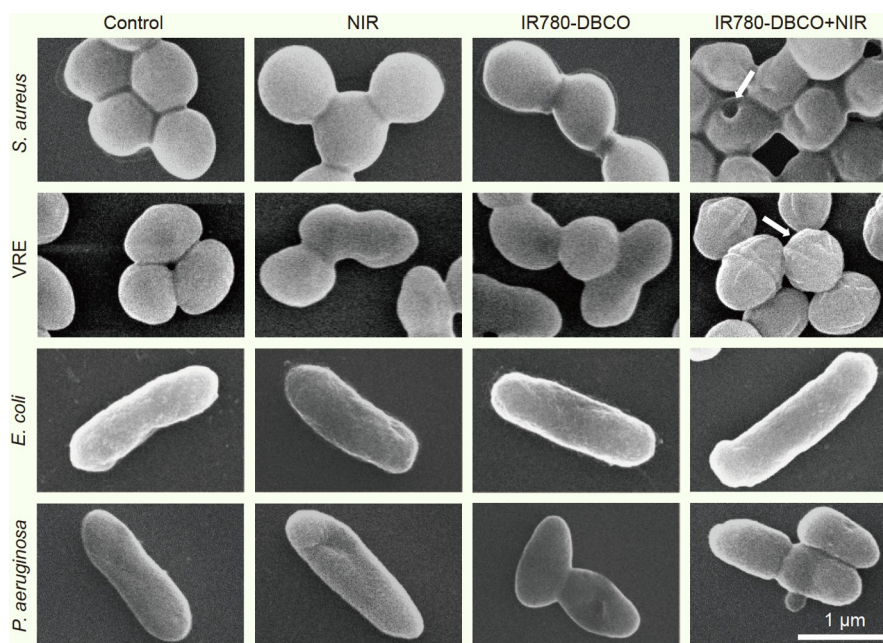


**Figure 6** SEM images of $D$-Ala-N$_3$-pretreated Gram-positive bacteria ($S.$ $aureus$ and VRE) and Gram-negative bacteria ($E.$ $coli$ and $P.$ $aeruginosa$) upon incubation with IR780-DBCO of $10\,\mu\mathrm{mol\,L^{-1}}$ and irradiation with/without 808-nm laser at a power density of $1.0\,\mathrm{W\,cm^{-2}}$ for 15 min.

smooth surface. These results clearly proved that IR780-DBCO conjugated on the bacterial surface could damage the integrity of bacterial cell walls through PTT [36,39], inducing the selective elimination of Gram-positive bacteria.

### *In vitro* biocompatibility study

To evaluate the potential of IR780-DBCO as a practical antimicrobial agent, the cytotoxicity of IR780-DBCO against mouse embryonic fibroblast cells (NIH3T3) was determined [40]. As shown by alamarBlue assay, IR780-DBCO exhibited negligible cytotoxicity even at a concentration of $10\,\mu mol\,L^{-1}$ (Fig. 7a). Moreover, on the basis of live/dead staining results, NIH3T3 cells incubated with IR780-DBCO were almost alive with analogous morphology to the control cells (Fig. 7b). In addition, blood compatibility of IR780-DBCO was assessed [41]. After incubating rabbit red blood cells (RBCs) with *D*-Ala-N$_3$ and different concentrations of IR780-DBCO, colorless supernatant similar to normal saline group was observed with the hemolysis ratios lower than 1% (Fig. 7c and Fig. S7). Nevertheless, the supernatant of RBCs treated with hemolytic 0.1% Triton X-100 showed a red color due to the rupture of cell membrane of RBCs and the release of a large amount of hemoglobin. These results indicated that IR780-DBCO had outstanding biocompatibility towards mammalian cells.

### *In vivo* anti-infective assay

To further demonstrate the bactericidal efficacy of IR780-DBCO *in vivo*, we established an animal model with azide-labelled VRE-infected wounds on the back skin of BALB/c mice. Upon different treatments with NIR light irradiation, IR780-DBCO, or IR780-DBCO plus NIR light irradiation, the photographs of wounds were recorded at varied time points. As depicted in Fig. 8a, all the VRE-infected wounds had a certain degree of suppuration on day 2. Moreover, compared with the groups with no treatment or treated with only NIR light irradiation or IR780-DBCO, the suppuration in the group treated with IR780-DBCO plus NIR light irradiation was obviously diminished on day 4, proving that IR780-DBCO was capable of inhibiting the bacterial infection at the wound site through PTT. Meanwhile, VRE in the homogenized wound tissues on day 4 was quantified to evaluate the anti-infective effect of IR780-DBCO. The number of bacteria in wound tissues for the control group, NIR light irradiation group, or IR780-DBCO group was $10.87 \times 10^6$, $8.97 \times 10^6$, or $6.30 \times 10^6\,CFU\,g^{-1}$, respectively, which was consistent with the result of a large amount of bacterial colonies presented on the agar plate (Fig. 8b, c). However, the bacterial number detected in IR780-DBCO plus NIR light irradiation treated group reduced by three orders of magnitude, with only $2.76 \times 10^3\,CFU\,g^{-1}$, which indicated the excellent photothermal bactericidal performance of IR780-DBCO. In addition, the wound tissues of mice were collected on day 4 and stained with H&E to investigate the anti-infective ability of IR780-DBCO towards VRE. Generally, infected tissues can generate large numbers of neutrophils, which are stained blue by H&E staining [42]. As revealed in Fig. 8d, VRE-infected wounds treated with IR780-DBCO plus NIR light irradiation showed much fewer neutrophils than the other groups, implying that IR780-DBCO under NIR laser illumination could significantly eliminate Gram-positive VRE
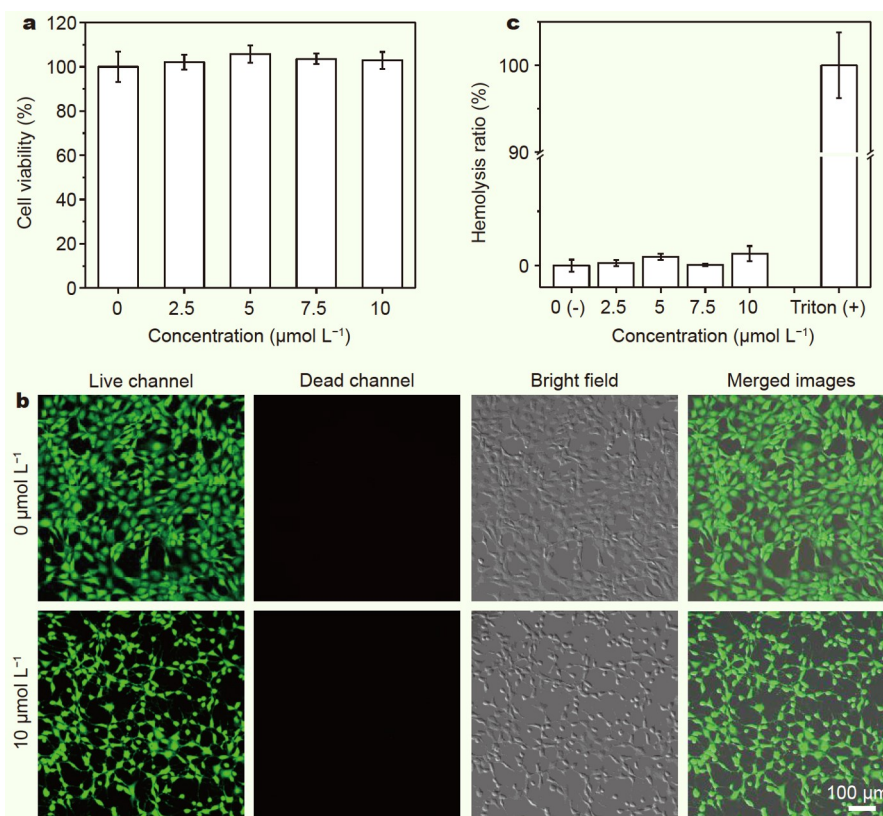


**Figure 7** (a) Cell viability and (b) live/dead staining of NIH3T3 cells cultured with *D*-Ala-N$_3$ and IR780-DBCO at different concentrations. (c) Hemolysis ratios of RBCs treated with *D*-Ala-N$_3$ and IR780-DBCO at different concentrations, 0.1% Triton X-100 (positive control), and normal saline (negative control). Error bars: mean ± SD ($n$ = 3).
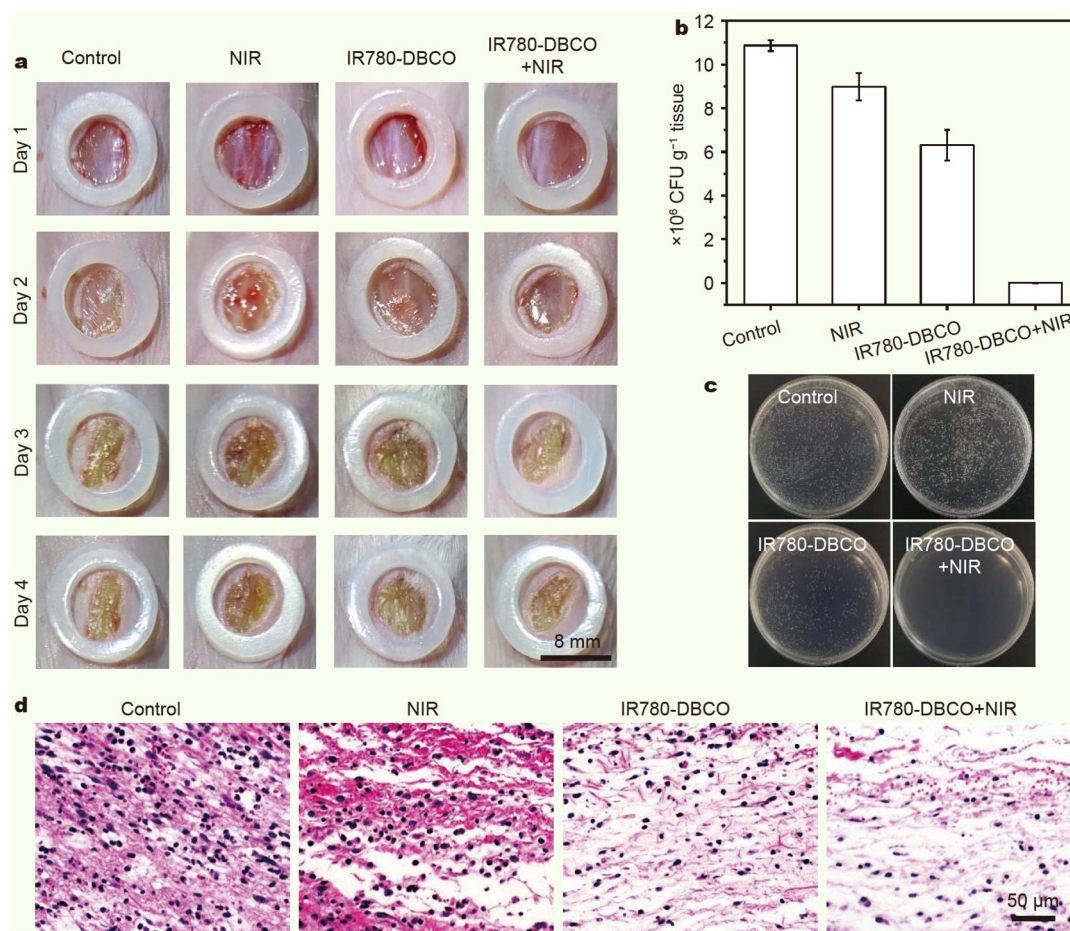
**Figure 8** (a) Photographs of VRE-infected wounds of mice with different treatments (Control, NIR light irradiation, IR780-DBCO, or IR780-DBCO plus NIR light irradiation) on days 1, 2, 3, and 4. (b) Quantitative analysis and (c) photographs of bacterial colonies from wound tissues of different treatment groups ($n$ = 3). (d) H&E-stained wound tissues after different treatments for four days.

and effectively suppress bacterial infection at the wounds.

## CONCLUSIONS

In summary, Gram-positive bacteria were selectively inactivated by a bioorthogonal photothermal agent (IR780-DBCO) *via* metabolic engineering. Followed by pretreating bacteria with metabolic precursor $D$-Ala-N$_3$, the bioorthogonal IR780-DBCO could be specifically conjugated on the surface of Gram-positive bacteria instead of Gram-negative ones through click reaction. Benefitting from the outstanding photothermal conversion performance and excellent biocompatibility of IR780-DBCO, precise inactivation of Gram-positive bacteria, such as *S. aureus* and superbug VRE, was demonstrated under NIR light irradiation. Most importantly, *in vivo* anti-infective capability was successfully verified in a VRE-infected mouse skin wound model. As compared with the reported nanoplatforms [43–45] or electrostatic and hydrophobic interaction-based strategies [46–48] for selective bacterial imaging and elimination, our method is advantageous in the stable covalent conjugation of photothermal agent on the cell wall with short distance for enhanced and spatiotemporally controlled PTT, as well as the defined or tunable chemical structures and the easy diffusion to infectious sites of small-molecule reagents. This study not only provides valuable practice for designing bioorthogonal photo-

thermal molecules and one-step metabolic labelling photo-theranostic agents to specifically sterilize Gram-positive bacteria, but also promotes the development of next-generation antimicrobial agents in the post-antibiotic era.

1 Casadevall A, Pirofski LA. Microbiology: Ditch the term pathogen. Nature, 2014, 516: 165–166

2 Rohr JR, Barrett CB, Civitello DJ, *et al.* Emerging human infectious diseases and the links to global food production. Nat Sustain, 2019, 2: 445–456

3 Menichetti F. Current and emerging serious Gram-positive infections. Clin Microbiol Infect, 2005, 11: 22–28

4 Chung HJ, Reiner T, Budin G, *et al.* Ubiquitous detection of Gram-positive bacteria with bioorthogonal magnetofluorescent nanoparticles. ACS Nano, 2011, 5: 8834–8841

5 Rhee C, Dantes R, Epstein L, *et al.* Incidence and trends of sepsis in US hospitals using clinical vs claims data, 2009–2014. J Am Med Assoc, 2017, 318: 1241–1249

6 Fleischmann C, Scherag A, Adhikari NKJ, *et al.* Assessment of global incidence and mortality of hospital-treated sepsis. Current estimates and limitations. Am J Respir Crit Care Med, 2016, 193: 259–272

7 Kollef MH. Broad-spectrum antimicrobials and the treatment of serious bacterial infections: Getting it right up front. Clin Infect Dis, 2008, 47:

S3–S13

8  Chellat MF, Raguž L, Riedl R. Targeting antibiotic resistance. Angew Chem Int Ed, 2016, 55: 6600–6626

9  Wang S, Xu M, Huang K, *et al.* Biocompatible metal-free organic phosphorescent nanoparticles for efficiently multidrug-resistant bacteria eradication. Sci China Mater, 2020, 63: 316–324

10  Levin-Reisman I, Ronin I, Gefen O, *et al.* Antibiotic tolerance facilitates the evolution of resistance. Science, 2017, 355: 826–830

11  Ma YX, Wang CY, Li YY, *et al.* Considerations and caveats in combating ESKAPE pathogens against nosocomial infections. Adv Sci, 2020, 7: 1901872

12  Yu F, Chen C, Yang G, *et al.* An acid-triggered porphyrin-based block copolymer for enhanced photodynamic antibacterial efficacy. Sci China Chem, 2021, 64: 459–466

13  Ye X, Feng T, Li L, *et al.* Theranostic platforms for specific discrimination and selective killing of bacteria. Acta Biomater, 2021, 125: 29–40

14  Ray PC, Khan SA, Singh AK, *et al.* Nanomaterials for targeted detection and photothermal killing of bacteria. Chem Soc Rev, 2012, 41: 3193–3209

15  Hsiao CW, Chen HL, Liao ZX, *et al.* Effective photothermal killing of pathogenic bacteria by using spatially tunable colloidal gels with nanolocalized heating sources. Adv Funct Mater, 2015, 25: 721–728

16  Korupalli C, Huang CC, Lin WC, *et al.* Acidity-triggered charge-convertible nanoparticles that can cause bacterium-specific aggregation *in situ* to enhance photothermal ablation of focal infection. Biomaterials, 2017, 116: 1–9

17  Chen Q, He S, Zhang F, *et al.* A versatile Pt-Ce6 nanoplatform as catalase nanozyme and NIR-II photothermal agent for enhanced PDT/PTT tumor therapy. Sci China Mater, 2021, 64: 510–530

18  Xu JW, Yao K, Xu ZK. Nanomaterials with a photothermal effect for antibacterial activities: An overview. Nanoscale, 2019, 11: 8680–8691

19  Zhao Y, Dai X, Wei X, *et al.* Near-infrared light-activated thermosensitive liposomes as efficient agents for photothermal and antibiotic synergistic therapy of bacterial biofilm. ACS Appl Mater Interfaces, 2018, 10: 14426–14437

20  Lei W, Ren K, Chen T, *et al.* Polydopamine nanocoating for effective photothermal killing of bacteria and fungus upon near-infrared irradiation. Adv Mater Interfaces, 2016, 3: 1600767

21  Wang H, Li X, Tse BWC, *et al.* Indocyanine green-incorporating nanoparticles for cancer theranostics. Theranostics, 2018, 8: 1227–1242

22  Cai Y, Si W, Huang W, *et al.* Organic dye based nanoparticles for cancer phototheranostics. Small, 2018, 14: 1704247

23  Wang H, Tang L, Liu Y, *et al. In vivo* targeting of metabolically labeled cancers with ultra-small silica nanoconjugates. Theranostics, 2016, 6: 1467–1476

24  Yuan Y, Xu S, Cheng X, *et al.* Bioorthogonal turn-on probe based on aggregation-induced emission characteristics for cancer cell imaging and ablation. Angew Chem Int Ed, 2016, 55: 6457–6461

25  Sun T, Yu SH, Zhao P, *et al.* One-step selective exoenzymatic labeling (SEEL) strategy for the biotinylation and identification of glycoproteins of living cells. J Am Chem Soc, 2016, 138: 11575–11582

26  Wang W, Lin L, Du Y, *et al.* Assessing the viability of transplanted gut microbiota by sequential tagging with D-amino acid-based metabolic probes. Nat Commun, 2019, 10: 1317

27  Wang W, Yang Q, Du Y, *et al.* Metabolic labeling of peptidoglycan with NIR-II dye enables *in vivo* imaging of gut microbiota. Angew Chem Int Ed, 2020, 59: 2628–2633

28  Hudak JE, Alvarez D, Skelly A, *et al.* Illuminating vital surface molecules of symbionts in health and disease. Nat Microbiol, 2017, 2: 1–8

29  Mao D, Hu F, Kenry F, *et al.* Metal-organic-framework-assisted *in vivo* bacterial metabolic labeling and precise antibacterial therapy. Adv Mater, 2018, 30: 1706831

30  Hu F, Qi G, Kenry G, *et al.* Visualization and *in situ* ablation of intracellular bacterial pathogens through metabolic labeling. Angew Chem Int Ed, 2020, 59: 9288–9292

31  Wu M, Qi G, Liu X, *et al.* Bio-orthogonal AIEgen for specific discrimination and elimination of bacterial pathogens *via* metabolic engineering. Chem Mater, 2020, 32: 858–865

32  Liang H, DeMeester KE, Hou CW, *et al.* Metabolic labelling of the carbohydrate core in bacterial peptidoglycan and its applications. Nat Commun, 2017, 8: 15015

33  Dumont A, Malleron A, Awwad M, *et al.* Click-mediated labeling of bacterial membranes through metabolic modification of the lipopolysaccharide inner core. Angew Chem Int Ed, 2012, 51: 3143–3146

34  Shieh P, Sloan Siegrist M, Cullen AJ, *et al.* Imaging bacterial peptidoglycan with near-infrared fluorogenic azide probes. Proc Natl Acad Sci USA, 2014, 111: 5456–5461

35  Yan F, Duan W, Li Y, *et al.* NIR-laser-controlled drug release from DOX/IR-780-loaded temperature-sensitive-liposomes for chemophotothermal synergistic tumor therapy. Theranostics, 2016, 6: 2337–2351

36  Qing G, Zhao X, Gong N, *et al.* Thermo-responsive triple-function nanotransporter for efficient chemo-photothermal therapy of multidrug-resistant bacterial infection. Nat Commun, 2019, 10: 4336

37  Kuang Y, Zhang K, Cao Y, *et al.* Hydrophobic IR-780 dye encapsulated in cRGD-conjugated solid lipid nanoparticles for NIR imaging-guided photothermal therapy. ACS Appl Mater Interfaces, 2017, 9: 12217–12226

38  Kuru E, Hughes HV, Brown PJ, *et al. In situ* probing of newly synthesized peptidoglycan in live bacteria with fluorescent *D*-amino acids. Angew Chem Int Ed, 2012, 51: 12519–12523

39  Wu F, Zheng H, Wang W, *et al.* Rapid eradication of antibiotic-resistant bacteria and biofilms by MXene and near-infrared light through photothermal ablation. Sci China Mater, 2021, 64: 748–758

40  Zhi Z, Su Y, Xi Y, *et al.* Dual-functional polyethylene glycol-*b*-polyhexanide surface coating with *in vitro* and *in vivo* antimicrobial and antifouling activities. ACS Appl Mater Interfaces, 2017, 9: 10383–10397

41  Yang C, Hu F, Zhang X, *et al.* Combating bacterial infection by *in situ* self-assembly of AIEgen-peptide conjugate. Biomaterials, 2020, 244: 119972

42  Zhu Y, Xu C, Zhang N, *et al.* Polycationic synergistic antibacterial agents with multiple functional components for efficient anti-infective therapy. Adv Funct Mater, 2018, 28: 1706709

43  Chen Z, Ji H, Liu C, *et al.* A multinuclear metal complex based DNase-mimetic artificial enzyme: Matrix cleavage for combating bacterial biofilms. Angew Chem Int Ed, 2016, 55: 10732–10736

44  Niu J, Sun Y, Wang F, *et al.* Photomodulated nanozyme used for a Gram-selective antimicrobial. Chem Mater, 2018, 30: 7027–7033

45  Sun Y, Zhao C, Niu J, *et al.* Colorimetric band-aids for point-of-care sensing and treating bacterial infection. ACS Cent Sci, 2020, 6: 207–212

46  Sayed SM, Xu KF, Jia HR, *et al.* Naphthalimide-based multifunctional AIEgens: Selective, fast, and wash-free fluorescence tracking and identification of Gram-positive bacteria. Anal Chim Acta, 2021, 1146: 41–52

47  Yang J, Gao G, Zhang X, *et al.* One-step synthesis of carbon dots with bacterial contact-enhanced fluorescence emission: Fast Gram-type identification and selective Gram-positive bacterial inactivation. Carbon, 2019, 146: 827–839

48  Zhang X, Chen X, Yang J, *et al.* Quaternized silicon nanoparticles with polarity-sensitive fluorescence for selectively imaging and killing Gram-positive bacteria. Adv Funct Mater, 2016, 26: 5958–5970

**Author contributions**    Feng T, Li P, and Huang W conceived the idea and supervised the study; Feng T, Ye X, and Lu H performed the experiments and wrote the manuscript; Nie C, Zhang J, Yu L, and Jin H participated in the *in vivo* anti-infective assay. All authors contributed to the general discussion.

**Conflict of interest**    The authors declare that they have no conflict of interest.

**Supplementary information**    Experimental details and supporting data are available in the online version of the paper.

**Tao Feng** received her BSc and MSc degrees from Jilin University in 2010 and 2013, and PhD degree from Nanyang Technological University in 2018. She is currently an associate professor at Northwestern Polytechnical University. Her research focuses on the design of fluorescent probes for selective discrimination and accurate killing of bacteria.

**Hui Lu** received his BSc degree from Anhui University of Technology in 2019. Currently, he is a graduate student at the Frontiers Science Center for Flexible Electronics, Northwestern Polytechnical University. His research interest is developing new phototheranostic agents to selectively inactivate bacteria.

**Xiaoting Ye** received her BSc degree from Nanjing Tech University in 2018 and MSc degree from the Frontiers Science Center for Flexible Electronics, Northwestern Polytechnical University in 2021. Her research focuses on preparing novel photothermal materials for specific killing of bacteria.

**Peng Li** received his BSc from Tianjin University in 2006 and PhD degree from Nanyang Technological University in 2013. He has been a professor of the Frontiers Science Center for Flexible Electronics at Northwestern Polytechnical University since 2018. His research interest is developing innovative antibacterial materials and strategies for infectious diseases.

**Wei Huang** received his BSc degree from Peking University in 1983, followed by MSc and PhD degrees from the same university. Then he did his postdoctoral research at the National University of Singapore, where he participated in the foundation of the Institute of Materials Research and Engineering in 1995. In 2011, he was elected as academician of the Chinese Academy of Sciences. Now, he is the chief scientist of the Frontiers Science Center for Flexible Electronics at Northwestern Polytechnical University. His research interests include polymer sciences, bioelectronics, nanoelectronics, and organic/plastic/flexible electronics.

## 代谢标记策略用于体外和体内革兰氏阳性菌的选择性杀灭

冯涛[1†*], 陆辉[1†], 叶晓婷[1†], 聂超凡[1], 张建红[1], 余骆峰[1], 靳昊宇[1], 李鹏[1*], 黄维[1,2,3]

**摘要**  细菌感染, 尤其是最常见的革兰氏阳性菌引起的感染, 严重威胁着人类的生命健康. 抗生素是治疗细菌感染的首选药物, 但是它的大量使用造成了耐药性细菌的快速滋生和蔓延. 近年来, 光热抗菌疗法作为一种不易引起细菌耐药性的技术受到了广泛的关注. 然而, 非特异性的细菌杀伤和对邻近哺乳动物细胞的毒副作用严重限制了光热抗菌疗法的实际应用. 本文开发了一种代谢标记策略用于革兰氏阳性菌的选择性光热杀灭. 通过二苯并环辛炔(DBCO)和IR-780碘化物的共价连接, 制备了生物正交的光热试剂IR780-DBCO. 革兰氏阳性菌或阴性菌经过3-叠氮基-D-丙氨酸预处理, 利用无铜点击化学反应实现了IR780-DBCO在金黄色葡萄球菌和耐万古霉素肠球菌等革兰氏阳性菌表面的选择性标记. 在15 min的近红外光照射下, 接近100%的革兰氏阳性菌被有效地杀灭. 此外, 该方法在小鼠皮肤伤口感染模型中也能够显著地抑制耐万古霉素肠球菌引起的感染. 我们提出的基于代谢标记的特异性光热杀灭革兰氏阳性菌的策略将会促进预临床研究中精准抗菌试剂的研发.